

# Cepstral Analysis of EEG During Visual Perception and Mental Imagery Reveals the Influence of Artistic Expertise

## Abstract

In this article, multichannel electroencephalogram (EEG) signals of artists and nonartists were analyzed during the performances of visual perception and mental imagery of paintings using cepstrum coefficients. Each of the calculated cepstrum coefficients and their parameters such as energy, average, standard deviation and entropy were separately used for distinguishing the two groups. It was found that a distinguishing coefficient might exist among the cepstrum coefficients, which could separate the two groups despite electrode placement. It was also observed that the two groups were distinguishable during the three states using the cepstrum coefficient parameters. However, separating the two groups was dependent on channel selection in this regard. The cepstrum coefficient parameters were found significantly lower for artists as compared to nonartists during the visual perception and the mental imagery, indicating a decreased average energy of EEG for artists. In addition, a similar significant decreasing trend in the cepstrum coefficient parameters was observed from occipital to frontal brain regions during the performances of the two cognitive tasks for the two groups, suggesting that visual perception and its mental imagery overlap in neuronal resources. The two groups were also classified using a neural gas classifier and a support vector machine classifier. The obtained average classification accuracies during the visual perception, the mental imagery, and at rest in the case of using the best selected distinguishable cepstrum coefficients were 76.87%, 77.5%, and 97.5%, respectively; however, a decrease in average recognition accuracy was found for classifying the two groups using the cepstrum coefficient parameters.

**Keywords:** Brain, cognition, electrodes, electroencephalography, entropy, paintings, support vector machine, visual perception

## Nasrin Shourie

Faculty of Technology and Engineering, Central Tehran Branch, Islamic Azad University, Tehran, Iran

## Introduction

Expertise and long-term training are attended by changes in certain aspects of brain activity while performing expertise-related tasks or processing expertise-related stimuli. Such differences are reflected in electroencephalogram (EEG) signals of experts.<sup>[1]</sup> Hence, EEG signals of professionals such as sportsmen and artists have been widely analyzed to date.<sup>[1-17]</sup> For instance, it has been found that professional marksmen exhibit significantly more alpha wave activity in left temporal, parietal, and occipital regions as compared to novices.<sup>[2,3]</sup> Crews *et al.*<sup>[4]</sup> have also observed that an increase in right-hemisphere alpha wave activity is related to decreased errors for expert golfers. An increased right-hemispheric alpha synchronization has been found for expert dancers as compared to novices during mental imagery of an improvisational dance.<sup>[5]</sup> It has been observed that musicians show an increased

alpha wave activity as compared to nonmusicians when passively listening to music.<sup>[6,7]</sup> Petsche *et al.*<sup>[8,9]</sup> have also found that musicians and nonmusicians are different in the levels of EEG coherence and beta wave activity plays a major role in the music processing. Pang *et al.*<sup>[10]</sup> have demonstrated that artistic expertise is related to decrease in event-related potential (ERP) responses to visual stimuli. Bhattacharya *et al.*<sup>[11]</sup> have found that phase synchrony significantly increased for artists as compared to nonartists in the high-frequency bands during visual perception. Karkar *et al.*<sup>[12]</sup> classified the EEG signals of the two groups using scaling exponents and a neural network-based classifier with an average recognition of 81.6%. Shourie *et al.*<sup>[13]</sup> have also investigated differences between artists and nonartists in scaling exponents during the performances of visual perception, mental imagery, and at rest. They have observed that the two groups are distinguishable at rest using scaling exponents;

## Address for correspondence:

Dr. Nasrin Shourie, Faculty of Technology and Engineering, Central Tehran Branch, Islamic Azad University, Tehran, Iran.  
E-mail: nas.shourie@iauctb.ac.ir

This is an open access article distributed under the terms of the Creative Commons Attribution-NonCommercial-ShareAlike 3.0 License, which allows others to remix, tweak, and build upon the work noncommercially, as long as the author is credited and the new creations are licensed under the identical terms.

For reprints contact: reprints@medknow.com

**How to cite this article:** Shourie N. Cepstral analysis of EEG during visual perception and mental imagery reveals the influence of artistic expertise. J Med Sign Sens 2016;6:203-17.

Website: www.jmss.mui.ac.ir

however, a decrease in average recognition accuracy has been found for classifying the two groups when performing the same cognitive tasks. It has also been shown that the two groups are distinguishable using wavelet coefficients. The average classification accuracies are 72.9%, 75%, and 100% for classification of the two groups during the visual perception, the mental imagery, and at the resting condition, respectively.<sup>[14]</sup> It has been observed that the alpha wave activity significantly decreases for artists as compared to nonartists during the two cognitive tasks.<sup>[15]</sup> A significant increased approximate entropy (ApEn) has been observed for artists as compared to nonartists during visual perception and mental imagery.<sup>[16]</sup>

This review of research indicates that brain activity analysis reflects the intensive training or education that experts received and prompted the current study, which classifies EEG signals of artists and nonartists. Hence, we explored the various EEG features and found that previous research has reported good results for classification of biological signals at various states using cepstral coefficients.

For instance, seizure and nonseizure EEG signals were classified using cepstral coefficients and a standard Gaussian mixture model with an average recognition of 91.7%.<sup>[17]</sup> Normal and epileptic EEG signals were also classified using cepstral-derived features and a neural network-based classifier with an average accuracy of 100%.<sup>[18,19]</sup> Other researchers have also shown the usefulness of cepstral-derived features for seizure detection.<sup>[20,21]</sup> Cepstral coefficients from the autoregressive (AR) model coefficients related to the movement-related EEG signals were calculated for classifying extension, flexion, and resting types of movement using a dynamic Hidden Markov Model-based (HMM) classifier, and an average recognition of 74.6% was achieved.<sup>[22]</sup> The usefulness of cepstral analysis for measuring the depth of anesthesia was shown.<sup>[23]</sup> Four types of emotions, happiness, fear, sadness, and calmness, were distinguished using Mel Frequency Cepstral coefficients and a multilayer perceptron (MLP)-based classifier with an average accuracy of 90%.<sup>[24]</sup> Mel frequency cepstral coefficients and K nearest neighbor (KNN) classifier were used for distinguishing different pairwise vowel imagery with an overall accuracy of 75%.<sup>[25]</sup> The usefulness of cepstral analysis for distinguishing between severity levels of speech impairment has also been shown.<sup>[26]</sup> It has been reported that cepstrum coefficients can provide a robust classification performance under disturbances such as variation in muscle contraction effort, muscle fatigue, and electromyogram (EMG) electrode location shift.<sup>[27]</sup> The usefulness of cepstrum technique for identification of the various heart problems has also been shown.<sup>[28-30]</sup> Five physiological variables (heart rate, blood temperature, oxygen saturation, systolic arterial blood pressure, and systolic pulmonary pressure) related to ill patients were investigated to classify them into two classes according

to the time they need to reach a stable state after coronary bypass surgery using cepstral coefficients, and the usefulness of cepstral analysis in this approach has been shown. Cepstral analysis was also used as an indirect measurement of heart rate for tachyarrhythmia detection.<sup>[30]</sup>

This review of research confirms the usefulness of cepstral analysis for classifying biological signals. However, there was no extensive research that investigated differences between the two groups in terms of cepstral coefficient parameters such as energy, mean, standard deviation (SD), and entropy (ENT). Therefore, our intention was to understand whether cepstral coefficients' differences could reflect artistic expertise. In this article, the two groups were compared during visual perception and mental imagery of some paintings. The effects of hemisphere (left vs. right) and region (frontal, centrottemporal, centroparietal, and occipital) were also considered. Results of this study may be used for measuring progress in novice artists.

We also used cepstrum coefficients' parameters for classifying EEG signals of artists and nonartists during visual perception, mental imagery, and resting condition. While each of the power cepstrum coefficients has a different meaning, it is likely that the two groups are also separable using some of the cepstrum coefficients. In addition, differences between the two groups may only be found in some of the channels. But, the best channels for distinguishing the two groups using cepstrum coefficient were not determined.

In this research, the best distinguishable cepstrum coefficient for each channel was selected using Davies–Bouldin index (DBI). Cepstrum coefficient parameters such as energy, mean, SD, and ENT were also calculated and the best distinguishable channels for each of them were determined. Finally, the two groups were classified using the best selected cepstrum coefficients and the cepstrum coefficient parameters during the three mentioned conditions.

## Materials and Methods

### Data set

This study analyzed the EEG signals that were recorded in a study by Bhattacharya *et al.* Twenty female participants were equally divided into two groups—professional artists and nonartists participated in this study. The artists (mean age 44.3 years old) graduated from the Vienna Academy of Fine Arts with an MA degree, and the nonartists (mean age 37.5 years old) had no specific interest or education in visual arts. Participants had to perform four tasks of visual perception (looking at a painting) and four tasks of mental imagery (mentally imagining the painting shown previously) of some paintings. Each task was repeated with four different paintings (painting 1: Bean-Festival by Jordaens, painting 2: an etching by Rembrandt, painting 3: an abstract painting by Kandinsky, and painting 4: a portrait by Holbein) for 2 min.

Each task was performed after a period of rest (1 min) and a distraction period of reading a newspaper article of neutral content [Figure 1].

The EEG signals were recorded by 19 electrodes (according to the international 10–20 system positions) with a sampling frequency of 128 Hz and a 12-bit A/D precision [Figure 2]. Electrode impedances were kept below 8 kΩ and the averaged signals of both earlobes were used as a reference.<sup>[11,12]</sup> The EEG signals were digitally filtered between 0.3 Hz and 45 Hz with a 6<sup>th</sup> order Butterworth band-pass filter and were also carefully checked for artifacts, and artifactual segments caused by eye blinks, eye movements, or muscle tension were eliminated.<sup>[16]</sup>

**Cepstral analysis**

The cepstrum of a signal is defined as the inverse Fourier transform of logarithmic magnitude of the spectrum.<sup>[30,31]</sup> The real cepstrum of signal  $x(t)$  was calculated as follows:

$$c(n) = \frac{1}{2\pi} \int_{-\pi}^{\pi} \log|X(\omega)| e^{j\omega n} d\omega \quad (1)$$

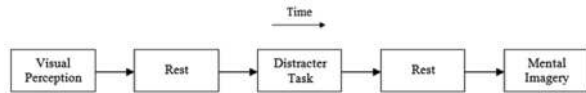


Figure 1: A schematic diagram related to one task of visual perception (2 min) corresponding one task of mental imagery (2 min). Each task was performed after a period of rest (1 min) and a distraction period of reading a newspaper article of neutral content (2 min)<sup>[12]</sup>

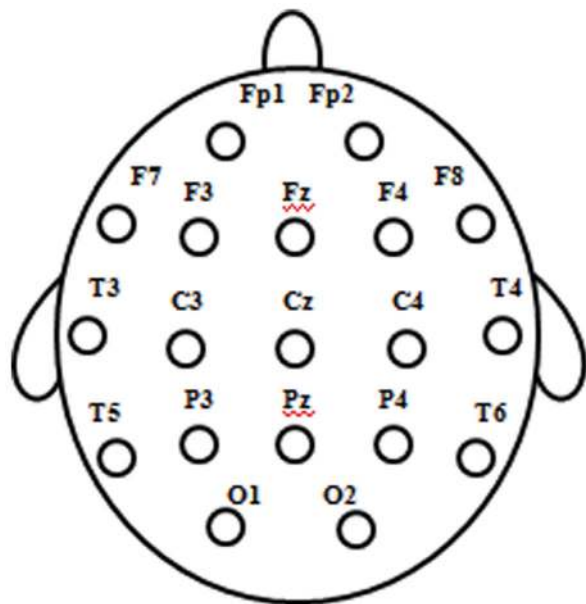


Figure 2: 19 electrode sites over the scalp according to the International 10–20 system. F refers to frontal, C for central, P for parietal, and O for occipital brain regions. Even electrodes are placed in the right hemisphere and odd electrodes are placed in the left hemisphere. The electrodes with a suffix z are placed in the midline zone<sup>[11]</sup>

The returned sequence  $c(n)$  is a real-valued vector, the same size as the input signal  $x$ , and  $X(\omega)$  is the Fourier transform of signal  $x$ . The power cepstrum was defined as follows:

$$\begin{aligned} c(n)^2 &= \left| \frac{1}{2\pi} \int_{-\pi}^{\pi} \log|X(e^{j\omega})| e^{j\omega n} d\omega \right|^2 \\ &= \frac{1}{2\pi} \int_{-\pi}^{\pi} \log|X(e^{j\omega})|^2 e^{j\omega n} d\omega \\ &= F^{-1} \{ \log(S(\omega)) \} \\ &= F^{-1} \{ \log(X(e^{j\omega})) \} \\ &\quad + F^{-1} \{ \log(X(e^{-j\omega})) \} \end{aligned} \quad (2)$$

where  $S(\omega)$  is the power spectrum of  $x$ . Each of the power cepstrum coefficients has a different meaning. For example,  $c(0)^2$  shows the average energy:

$$c(0)^2 = \frac{1}{2\pi} \int_{-\pi}^{\pi} \log S(\omega) d\omega \quad (3)$$

Finer details of the spectrum shape are represented by higher cepstral coefficients.

The real cepstrum is related to the power cepstrum via the relationship  $2 \times \text{real cepstrum} = \text{power cepstrum}$ .

In this research, real cepstrum coefficient parameters such as energy ( $E$ ), mean ( $M$ ), SD, and ENT were also computed for investigating the effect of art training in the EEG signals. The cepstrum coefficient energy ( $E$ ) was calculated by the following equation:

$$E = \sum_{n=1}^N |c(n)|^2 \quad (4)$$

where  $N$  is the number of cepstrum coefficients. The cepstrum coefficient mean ( $M$ ) was calculated using the following equation:

$$M = \frac{1}{N} \sum_{n=1}^N c(n) \quad (5)$$

The cepstrum coefficient SD was calculated as follows:

$$SD = \left( \frac{1}{N-1} \sum_{n=1}^N (c(n) - \mu)^2 \right)^2 \quad (6)$$

The cepstrum coefficient ENT was calculated using the following equation:

$$ENT = - \sum_{n=1}^N c(n)^2 \log(c(n)^2) \quad (7)$$

**Statistical analysis**

A series of 4×2×4×2 (PAINTING×HEMISPHERE×REGION×GROUP) analysis of variances (ANOVAs) with repeated measures were computed to determine whether the differences in the cepstrum coefficient parameters among the variables were significant. The PAINTING variable consisted of four paintings that participants had to look at and then imagine. The HEMISPHERE variable referred to two levels: left and right (the midline electrodes (Pz, Cz, Fz) were not included). The REGION variable consisted of four levels as follows: frontal (Fp1, F3, F7, Fp2, F4, F8), centrottemporal (C3, T3, C4, T4), parietotemporal (P3, T5, P4, T6), and occipital (O1, O2). The GROUP variable referred to two levels: artist and nonartist. Huynh–Feldt procedure was used to correct sphericity assumptions degrees of freedom, and Bonferroni method was used for multiple comparisons. The repeated measure ANOVAs were computed separately for the visual perception and the mental imagery tasks.<sup>[13]</sup>

**Davies–Bouldin index**

The DBI is a metric for cluster validity and measures discriminability between clusters, which is designed based on scattering matrices. A lower DBI indicates more discriminability between the clusters. Conversely, a higher DBI shows more similarity between the clusters. The DBI calculation procedure can be expressed as follows:<sup>[32]</sup>

$$DB = \frac{1}{C} \sum_{i=1}^C D_i \tag{8}$$

where  $C$  is the number of clusters and  $D_i$  is equal to  $R_{i,j}$  for the most similar cluster to cluster  $i$  as follows:

$$D_i = \max_{i:i \neq j} R_{i,j} \tag{9}$$

where  $R_{i,j}$  is the similarity between cluster  $i$  and  $j$  and is calculated using the following equation:

$$R_{i,j} = \frac{S_i + S_j}{M_{i,j}} \tag{10}$$

where  $S_i$  is a measure of within cluster scatter for cluster  $i$ , and  $M_{i,j}$  is a measure of separation between the  $i^{\text{th}}$  and the  $j^{\text{th}}$  clusters.

$$M_{i,j} = \|Z_i - Z_j\|_p \tag{11}$$

$$S_i = \left[ \frac{1}{J} \sum_{j=1}^{J_i} \|X_j - Z_i\|^q \right]^{1/q} \quad X_j \in \text{cluster } i \tag{12}$$

where  $Z_i$  is the centroid of cluster  $i$ , and  $J_i$  is the size of cluster  $i$ . In this research,  $p$  and  $q$  are set to 2.

The range of classification accuracy may be predicted using DBI. In this approach, if the calculated DBI was lower than 2.5, one can expect that classification accuracy was more than 60%. If the DBI was lower than 1, then the recognition accuracy might be more than 90%.<sup>[14]</sup>

**Classification**

*Neural gas classifier*

Neural gas is a competitive network in that it has no certain topology. The number of its neurons is constant during a learning procedure. The neurons of the network are adapted according to their distance to training data. The neural gas algorithm can be summarized as shown below:<sup>[33,34]</sup>

1 – Initialize the neurons’ set  $A$  with  $N$  neurons:

$$A = \{c_1, c_2, \dots, c_N\} \tag{13}$$

Each neuron has a reference vector  $w$  that is chosen randomly.

2 – Calculate the distance between a training input  $\zeta$  and each neuron.

3 – Order all neurons of  $A$  according to their distance to a training input  $\zeta$ . It means that the sequence of indices ( $i_1, i_2, \dots, i_{N-1}$ ) should be found such that  $w_{i_1}$  is the closest reference vector to  $\zeta$ ,  $w_{i_2}$  is the second closest reference vector to  $\zeta$  and  $w_{i_k}$ , and  $k = 0, 1, \dots, N-1$  is the  $k^{\text{th}}$  reference vector close to  $\zeta$ .

4 – Update the reference vectors as shown below:

$$\Delta w_i = \epsilon(t) \cdot b_\lambda(k_i(\zeta, A)) \cdot (\zeta - w_i) \tag{14}$$

$$\lambda(t) = \lambda_i (\lambda_f / \lambda_i)^{t/t_{\max}} \tag{15}$$

$$\epsilon(t) = \epsilon_i (\epsilon_f / \epsilon_i)^{t/t_{\max}} \tag{16}$$

$$b_\lambda(k) = \exp(-k/\lambda(t)) \tag{17}$$

5 – Increase the time parameter  $t$ .

6 – If  $t < t_{\max}$ , continue with step 2.

After training, the neurons cover the space of the training data. For classification of an unknown input, its distances to all of the neurons should be calculated. The label of the closest neuron to the unknown input determines its label.<sup>[14]</sup>

*SVM Classifier*

The linear support vector machine (SVM) is a classification algorithm that distinguishes two groups using a separating hyperplane in the training data space and by penalizing mistakenly classified data points. The two groups are divided by a clear gap that is as wide as possible. An unknown input is then mapped into that same space and predicted to belong to a category based on which side of the gap they fall on.<sup>[35]</sup>

**Results**

**Statistical analysis**

The three cepstrum coefficient parameters were calculated for the EEG signals of the two groups during the performances of the visual perception tasks and the mental imagery tasks. A series of  $4 \times 2 \times 4 \times 2$  (PAINTING  $\times$  HEMISPHERE  $\times$  REGION  $\times$  GROUP) ANOVAs with repeated measures were computed to determine the significant differences in the cepstrum coefficient parameters between the variables. The obtained results are shown in Figures 3–8.

In the cepstrum coefficient energy related to the visual perception tasks, a significant main effect REGION ( $F = 20.18, P < 0.001$ ) was observed, indicating a decrease in cepstrum coefficient energy from occipital to

frontal brain regions. This effect was more pronounced for nonartists; however, this interaction between REGION and GROUP failed to reach statistical significance ( $F = 1.63, P = 0.18$ ). We also found a significant main effect GROUP with lower cepstrum coefficient energy for artists ( $F = 8.41, P < 0.01$ ). The remaining ANOVA effects in the cepstrum coefficient energy were not significant [Figure 3].

In the cepstrum coefficient mean related to the visual perception tasks, a significant main effect REGION was found, indicating a decrease in cepstrum coefficient mean from parietotemporal to frontal brain regions ( $F = 7.42, P < 0.001$ ). This effect was more pronounced for artists. We also observed a significant main effect GROUP, suggesting that artists displayed a lower cepstrum coefficient mean as compared to nonartists ( $F = 9.30, P < 0.01$ ). Artists and nonartists exhibited different variation patterns of cepstrum coefficient mean during the visual perception tasks. This effect is evidenced by a significant interaction between PAINTING, REGION, and GROUP ( $F = 2.05, P < 0.05$ ). The remaining ANOVA effects in the cepstrum coefficient mean were not significant [Figure 4].

In the cepstrum coefficient Std related to the visual perception tasks, a significant main effect REGION was found, suggesting a decrease in cepstrum coefficient Std from occipital to frontal brain regions ( $F = 17.13, P < 0.001$ ). In addition, a significant

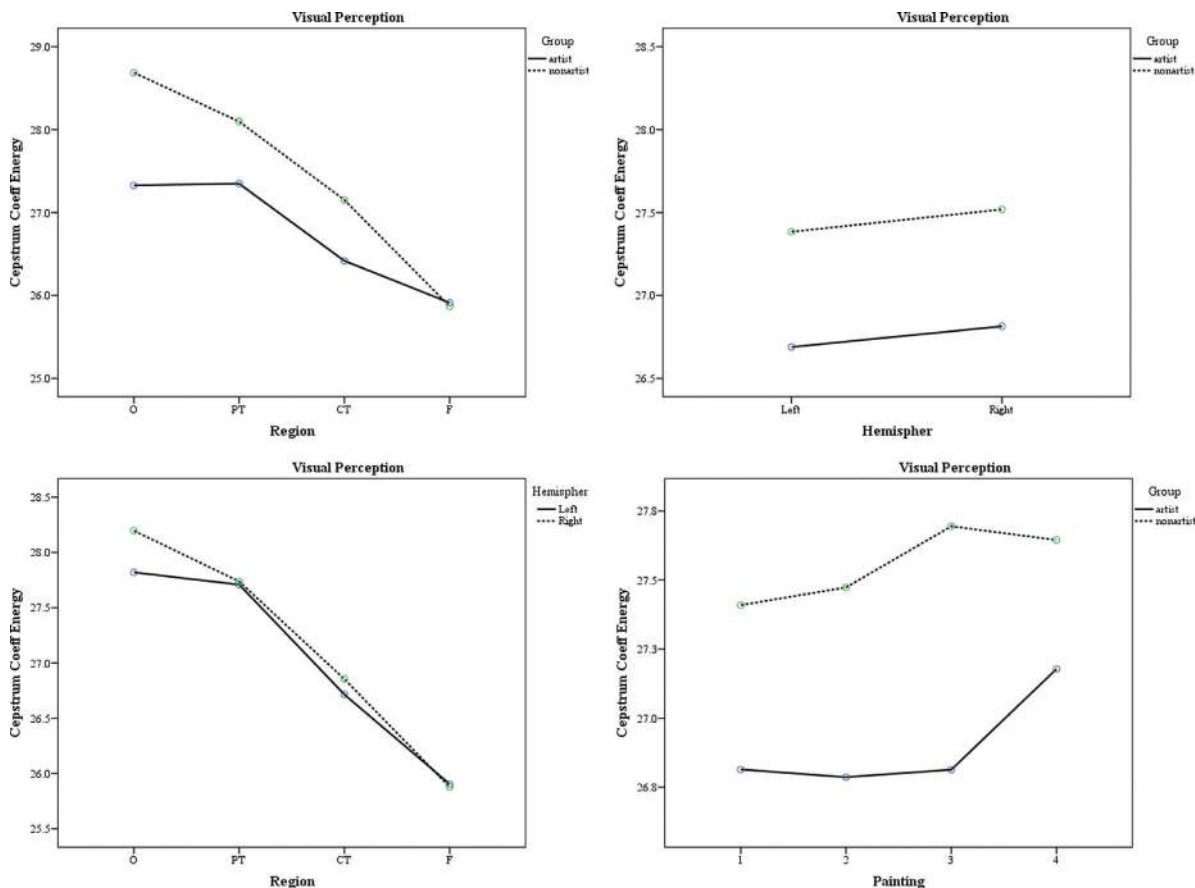


Figure 3: Changes in EEG cepstrum coefficient energy during visual perception

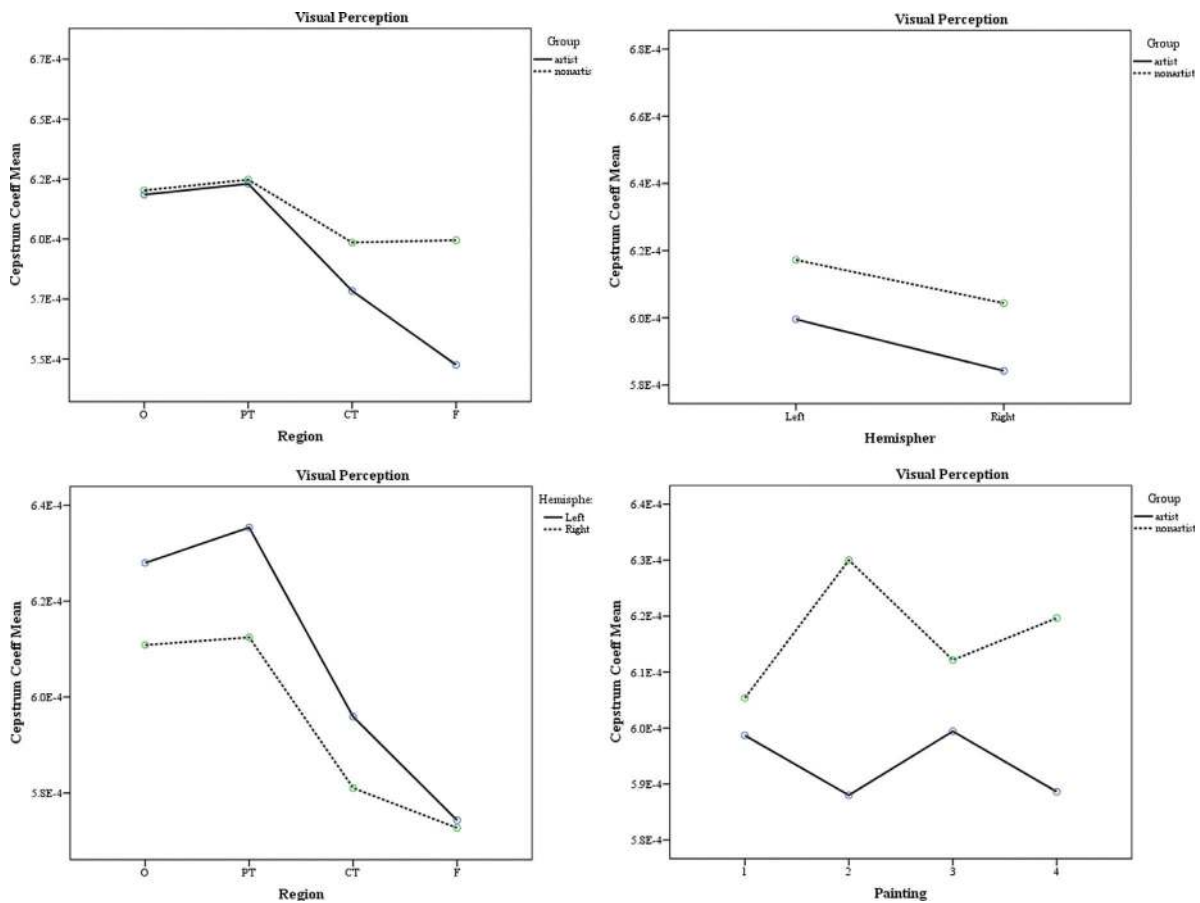


Figure 4: Changes in EEG cepstrum coefficient mean during visual perception

main effect GROUP was observed with lower cepstrum coefficient Std for artists as compared to nonartists ( $F = 10.26, P < 0.01$ ). The remaining ANOVA effects in the cepstrum coefficient Std failed to reach statistical significance [Figure 5]. The cepstrum coefficient parameter was averaged across the four trials of the two groups during the visual perception and is shown in Figure 6.

In the cepstrum coefficient energy related to the mental imagery tasks, a significant main effect PAINTING was observed ( $F = 4.48, P < 0.01$ ). Artists and nonartists exhibited different patterns of cepstrum coefficient energy during visualization of the four paintings. This effect was evidenced by a significant interaction between PAINTING and GROUP ( $F = 9.84, P < 0.001$ ). In addition, a significant main effect REGION was found ( $F = 17.22, P < 0.001$ ), indicating a decrease in cepstrum coefficient energy from parietotemporal to frontal brain regions. A significant main effect GROUP with lower cepstrum coefficient energy was also observed for artists ( $F = 5.75, P < 0.05$ ). The remaining ANOVA effects in the cepstrum coefficient energy were not significant [Figure 7].

In the cepstrum coefficient mean during the mental imagery tasks, a significant main effect REGION was found ( $F = 3.10, P < 0.05$ ), indicating an increased cepstrum coefficient mean in parietotemporal brain region.

In addition, a significant interaction between PAINTING and REGION was observed ( $F = 793.5, P < 0.01$ ). This effect was further moderated by GROUP (PAINTING  $\times$  REGION  $\times$  GROUP interaction:  $F = 974.0, P < 0.05$ ). Artists tend to show a different pattern of cepstrum coefficient mean as compared to nonartists; however, the main effect GROUP failed to reach statistical significance ( $F = 2.56, P = 0.11$ ). The remaining ANOVA effects were not significant [Figure 8].

In the cepstrum coefficient Std during the mental imagery tasks, a significant main effect PAINTING was observed ( $F = 4.35, P < 0.01$ ), indicating that artists and nonartists showed different patterns of cepstrum coefficient Std when visualizing the different paintings. This was suggested by a significant interaction between PAINTING and GROUP ( $F = 7.33, P < 0.001$ ). Artists displayed lower cepstrum coefficient Std as compared to nonartists (main effect GROUP:  $F = 7.80, P < 0.01$ ). In addition, a significant main effect REGION was observed, indicating a decrease in cepstrum coefficient Std from occipital to frontal brain regions ( $F = 20.11, P < 0.001$ ). The remaining ANOVA effects were not significant [Figure 9]. The cepstrum coefficient parameter was averaged across the four trials of the two groups during the mental imagery and shown in Figure 10. Summary of ANOVA effects is also shown in Table 1.

**Davies–Bouldin’s index calculation**

The cepstrum coefficients were calculated for the EEG signals of the two groups during the visual perception, the mental imagery, and at the resting condition. Then, the cepstrum coefficient parameters (energy, mean, SD, and ENT) were calculated for the obtained cepstrum coefficient. DBI was calculated for cepstrum coefficient parameters of each channel separately. The obtained results are shown in Table 2, and the best distinguishable channels (with the lowest DBI) are highlighted.

As shown in Table 2, it was found that the two groups are distinguishable during the three states using the cepstrum coefficient parameters. But, the separation of the two groups was dependent on channel selection. This was because DBI was obtained higher than 3 for some channels, and therefore, these channels are not appropriate for distinguishing the two groups. In addition, DBI decreases at the resting condition as compared to the visual perception and the mental imagery. Therefore, it was expected that the average classification accuracy of the two groups at the resting condition must be higher.

Next, DBI was calculated for each of the obtained cepstrum coefficient. Then, the cepstrum coefficient with the lowest value in the DBI was determined for each of the tasks and channels separately. The obtained results are shown in Table 3, and the indices of the best distinguishing cepstrum coefficients were noted.

As shown in Table 3, no noticeable differences were observed between the different channels and DBI was obtained lower than 3 for all channels and the three conditions. Therefore, a distinguishing cepstrum coefficient may exist among the

**Table 1: Summary of ANOVA effects**

ANOVAs	Task					
	Visual perception			Mental imagery		
	Energy	Mean	Std	Energy	Mean	Std
P	n.s.	n.s.	n.s.	**	n.s.	**
P × H	n.s.	n.s.	n.s.	n.s.	n.s.	n.s.
P × R	n.s.	n.s.	n.s.	n.s.	**	n.s.
P × G	n.s.	n.s.	n.s.	***	n.s.	***
P × H × R	n.s.	n.s.	n.s.	n.s.	n.s.	n.s.
P × H × G	n.s.	n.s.	n.s.	n.s.	n.s.	n.s.
P × R × G	n.s.	*	n.s.	n.s.	*	n.s.
P × H × R × G	n.s.	n.s.	n.s.	n.s.	n.s.	n.s.
H	n.s.	n.s.	n.s.	n.s.	n.s.	n.s.
R	***	***	***	***	*	***
G	**	**	**	*	n.s.	**
H × R	n.s.	n.s.	n.s.	n.s.	n.s.	n.s.
H × G	n.s.	n.s.	n.s.	n.s.	n.s.	n.s.

P = PAINTING, H = HEMISPHERE, R = REGION, G = GROUP, n.s. = not significant, \*  $P < 0.05$ , \*\*  $P < 0.01$ , \*\*\*  $P < 0.001$ .

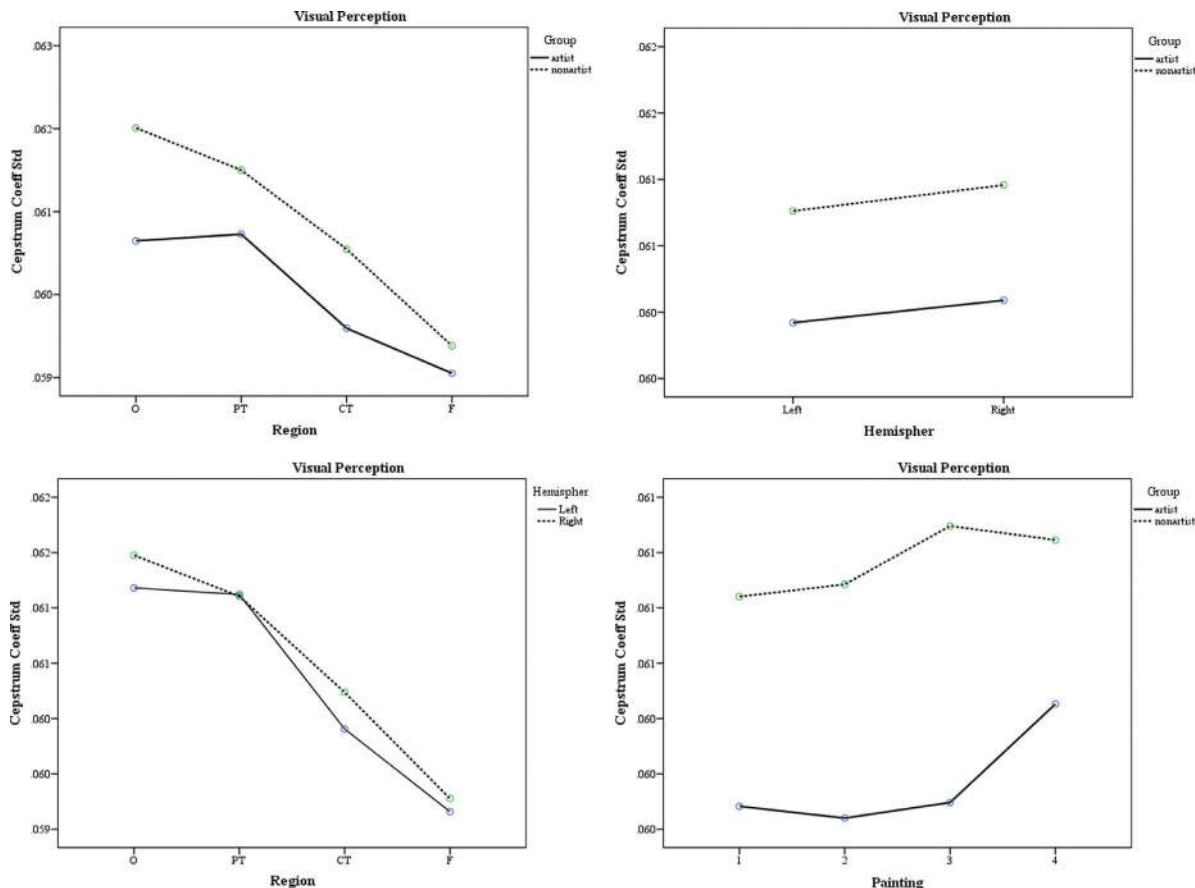


**Figure 5: Changes in EEG cepstrum coefficient Std during visual perception**

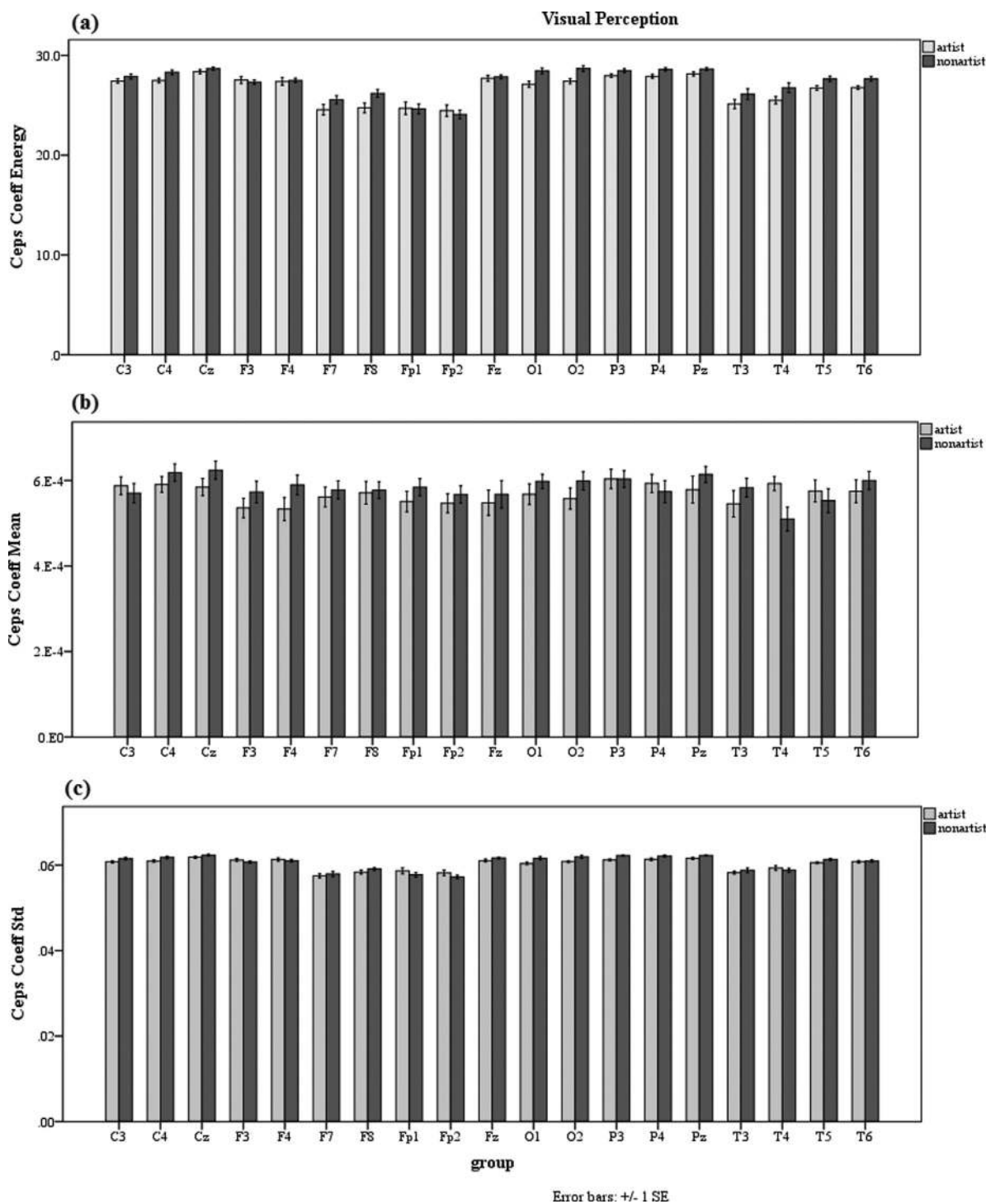


Figure 6: The cepstrum coefficients: (a) energy, (b) mean, and (c) Std averages of the two groups across the four trials during the visual perception

cepstrum coefficients that can discriminate the two groups despite the placement of the electrode.

### Classification of the EEG signals

In this research, the two groups were classified using cepstrum coefficient parameters in their corresponding selected channels and a SVM and a neural gas classifier separately. For instance, in the case of the visual perception,

the greatest discriminability was observed in Fz channel for the cepstrum coefficient mean and O2 for the remaining cepstrum coefficient parameters [Table 1]. Therefore, O2 and Fz channels were selected for classifying the two groups during the visual perception. For each classification, the calculated features were permuted and divided into two groups: training data (80%) and test data (20%). Finally, for each feature and state, the averaged sensitivity



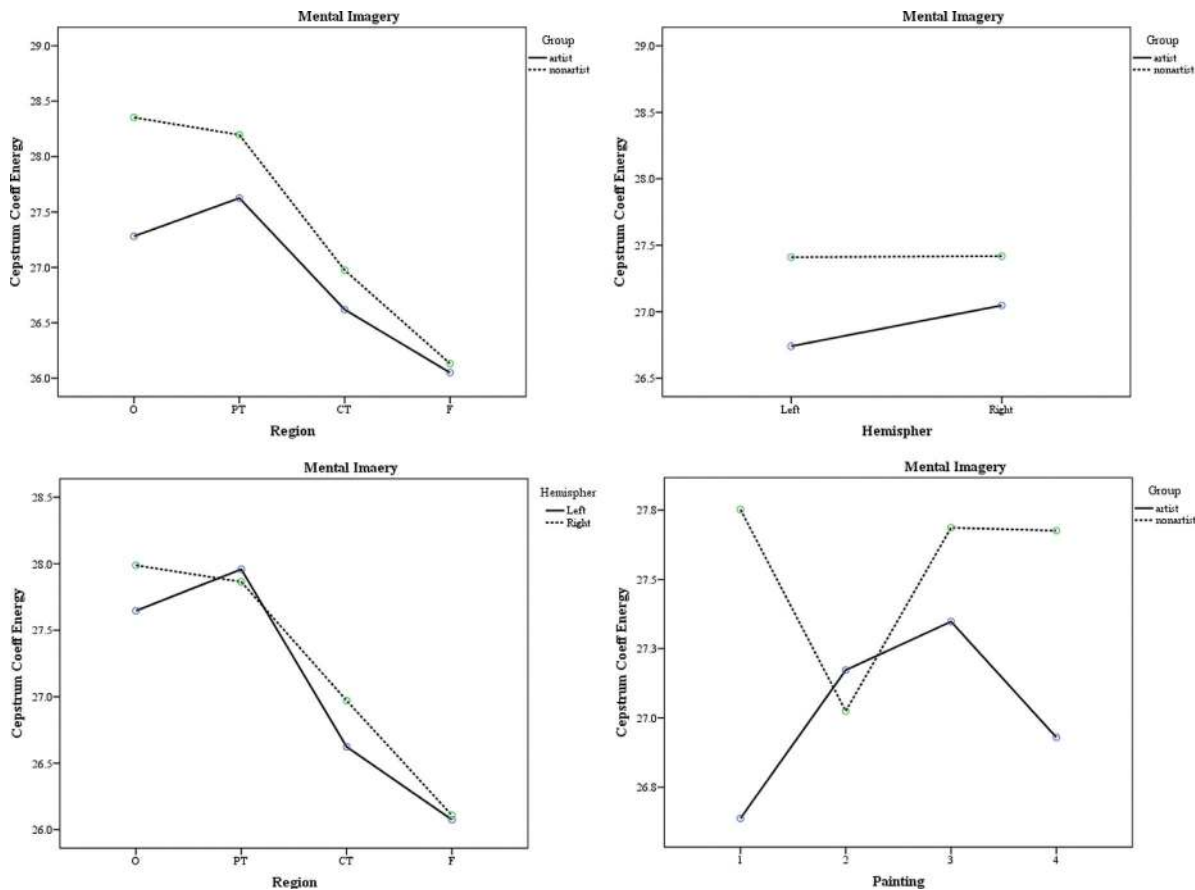


Figure 7: Changes in EEG cepstrum coefficient energy during mental imagery

Table 2: The Davies–Bouldin index values for the average, the standard deviation (SD), the energy, and the entropy (ENT) of the cepstrum coefficients related to the two groups during the visual perception, the mental imagery, and at the resting condition

CH	Visual perception				Mental imagery				Rest			
	Energy	Mean	SD	ENT	Energy	Mean	SD	ENT	Energy	Mean	SD	ENT
Fp1	31.869	10.190	43.468	20.891	8.1766	8.1986	8.7182	7.0076	60.040	22.022	175.74	40.467
Fp2	17.066	4.4295	19.729	12.548	5.9781	12.893	6.2352	5.3145	15.799	5.3150	20.658	10.841
F7	7.0911	12.542	6.9128	7.0175	14.933	16.790	16.795	15.576	3.7560	20.817	3.8048	3.8925
F3	157.96	23.071	452.72	38.217	13.520	8.1697	14.995	10.428	7.8411	12.484	8.6594	6.9754
Fz	20.508	<b>2.4520</b>	18.740	53.745	26.351	6.7521	26.788	80.239	36.393	10.202	27.182	90.752
F4	46.032	2.7493	64.395	17.003	15.771	5.5057	17.072	10.522	53.194	7.9117	74.845	25.591
F8	3.8712	8.1946	3.8422	3.8372	71.499	47.094	120.21	291.09	24.344	2.1130	19.995	30.214
T3	6.4292	28.769	6.5359	7.1081	10.539	<b>6.1303</b>	11.784	11.506	5.3471	6.5865	5.3310	5.4906
C3	4.4954	9.7175	4.5443	4.8079	5.0686	15.538	5.1570	5.2232	4.5174	1.9799	4.4605	4.4264
Cz	7.6161	4.1336	7.5058	8.5691	4.9958	6.4830	4.9333	4.9729	5.3220	3.5353	5.1022	4.7724
C4	3.6359	4.5171	3.6386	3.8588	4.2789	10.134	4.3411	4.4109	12.004	20.712	12.053	20.080
T4	56.035	28.121	44.732	136.99	11.924	3.9724	12.114	9.6188	5.8162	4.6961	5.3288	4.7918
T5	3.5263	27.811	3.5375	3.4900	3.7911	98.311	3.8165	3.6528	3.7877	15.509	3.7696	4.2612
P3	4.7436	14.968	4.7330	5.3411	4.0273	14.140	4.1614	3.8111	3.2052	43.238	3.2025	3.1463
Pz	4.5659	12.013	4.4854	4.5574	3.9524	177.04	3.8833	4.1561	8.8407	<b>1.8525</b>	8.5426	10.384
P4	3.1561	17.201	3.1438	3.4136	4.1571	15.483	4.0746	4.2848	4.9862	3.6637	4.9954	4.9674
T6	2.9693	9.5886	2.9750	3.1828	10.107	13.380	10.304	11.250	1323.7	5.6744	418.13	30.573
O1	2.7829	25.454	2.7623	2.6765	3.4482	8.5563	3.5078	3.6284	<b>1.8178</b>	3.0328	<b>1.8129</b>	<b>1.8164</b>
O2	<b>2.7221</b>	37.543	<b>2.7287</b>	<b>2.5892</b>	<b>3.1311</b>	11.323	<b>3.2021</b>	<b>3.1287</b>	3.9278	2.0286	4.0059	4.4301

The best distinguishable channels (with the lowest DBI) are in bold

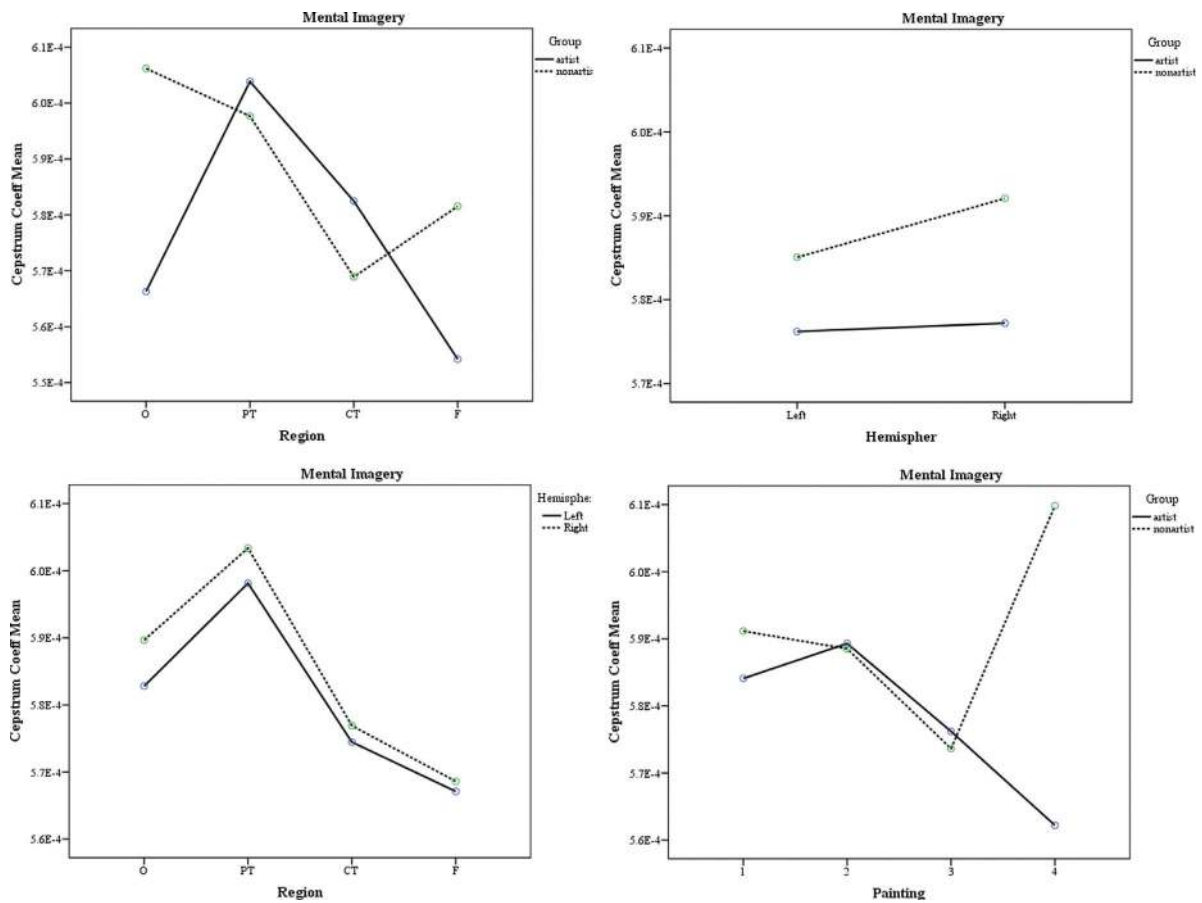


Figure 8: Changes in EEG cepstrum coefficient mean during mental imagery

**Table 3: The cepstrum coefficients with the lowest Davies–Bouldin index values for each of the channels**

CH	Visual perception		Mental imagery		Rest	
	Index	DB	Index	DB	Index	DB
Fp1	4	<b>1.7244</b>	1963	2.3984	2313	0.9777
Fp2	4523	2.2212	317	2.4476	6842	0.9830
F7	1913	2.1610	7422	2.1868	3501	0.9265
F3	3083	2.3255	423	2.0644	3937	0.6351
Fz	3055	2.4511	4357	2.1377	1493	0.9165
F4	4	2.0236	4698	2.3109	1027	0.8601
F8	7422	2.2695	27	2.0946	6842	0.8771
T3	4	2.1680	7417	1.7977	31	0.8319
C3	2966	1.7475	2242	2.0153	5740	0.8031
Cz	6394	2.3689	2028	2.1653	3700	0.8304
C4	7060	2.2094	3532	2.2369	3654	0.7946
T4	7422	2.0325	6715	2.1088	4813	0.9310
T5	40	2.0733	13	1.8468	3286	0.7653
P3	7413	2.0215	7418	1.8074	5942	0.8854
Pz	13	1.9287	8	1.9683	3353	0.9318
P4	7413	1.9173	7418	2.0538	285	0.8676
T6	166	1.7733	13	1.6861	7317	0.8542
O1	684	2.0165	7418	<b>1.6797</b>	38	0.9606
O2	13	1.9417	7418	1.7973	1957	<b>0.6399</b>

The best distinguishable channels (with the lowest DBI) are in bold

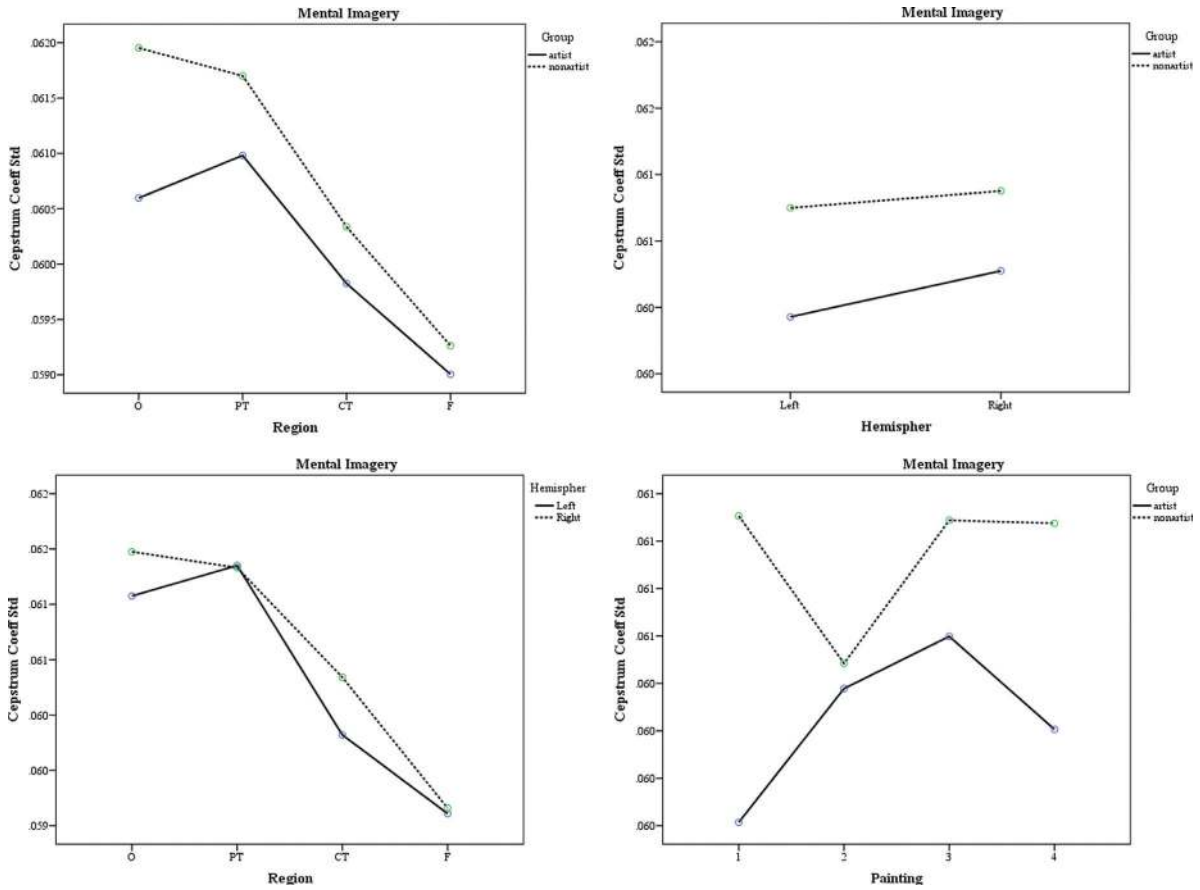


Figure 9: Changes in EEG cepstrum coefficient Std during mental imagery

Table 4: The results of classifying the two groups using SVM classifier

Cepstrum parameter	Task											
	Visual perception				Mental imagery				Rest%			
	CH	TPR	SPC	ACC	CH	TPR	SPC	ACC	CH	TPR	SPC	ACC
Energy	O2	86.25	45	65.62	O2	56.25	75	65.62	O1	80	90	<b>85</b>
Mean	Fz	86.25	53.75	<b>70</b>	T3	60	61.25	60.62	Pz	90	60	75
SD	O2	73.75	56.25	65	O2	63.75	68.75	66.25	O1	75	85	80
ENT	O2	67.5	56.5	62	O2	57.5	76.25	<b>68.87</b>	O1	85	75	80

The bold entries indicate the most obtained classification accuracy for each of the condition (visual perception, mental imagery and rest).

Table 5: The results of classifying the two groups using neural gas classifier

Cepstrum parameter	Task											
	Visual perception				Mental imagery				Rest%			
	CH	TPR	SPC	ACC	CH	TPR	SPC	ACC	CH	TPR	SPC	ACC
Energy	O2	87.5	56.25	<b>71.87</b>	O2	58.75	71.25	65	O1	65	80	72.5
Mean	Fz	78.75	65	<b>71.87</b>	T3	65	51.25	58.12	Pz	80	80	<b>80</b>
SD	O2	85	58.75	<b>71.87</b>	O2	76.25	66.25	<b>71.25</b>	O1	70	85	77.5
ENT	O2	70	63.75	66.87	O2	55	60	57.5	O1	70	70	70

The bold entries indicate the most obtained classification accuracy for each of the condition (visual perception, mental imagery and rest).

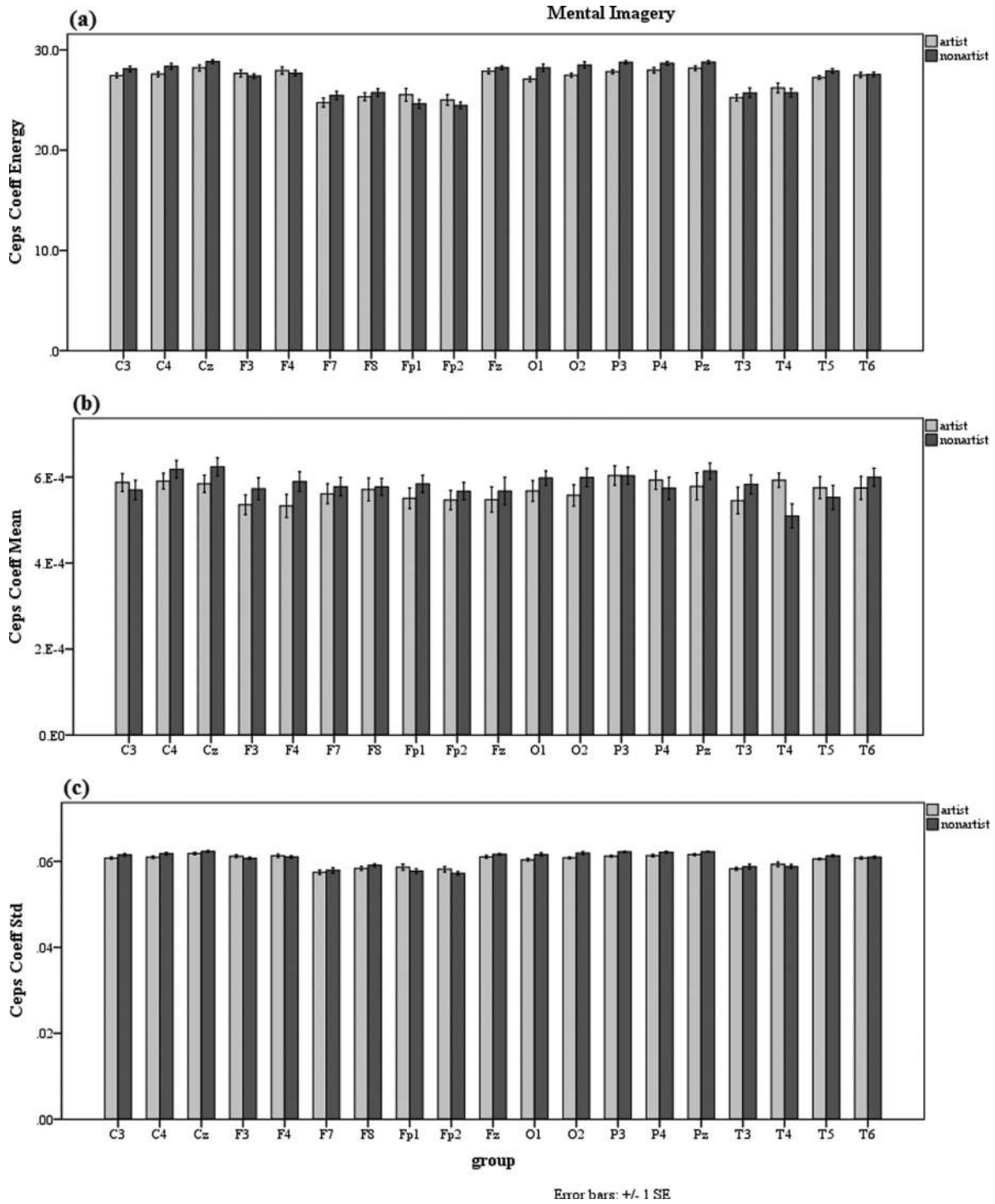


Figure 10: The cepstrum coefficients: (a) energy, (b) mean, and (c) Std averages of the two groups across the four trials during the mental imagery

(true positive rate), specificity (true negative rate), and accuracy (true decision rate) across ten separate classifications were calculated using the following equations:

$$TPR = \frac{TP}{TP + FN} \quad (18)$$

$$SPC = \frac{TN}{TN + FP} \quad (19)$$

$$ACC = \frac{TP + TN}{TP + TN + FP + FN} \quad (20)$$

where TPR, SPC, and ACC represent sensitivity, specificity, and accuracy, respectively. In addition, positive referred to identified (artist) and negative referred to rejected (nonartist) (True positive (TP)= correctly identified, False positive

(FP) = incorrectly identified, True negative (TN) = correctly rejected, and False negative (FN) = incorrectly rejected). The obtained results are shown in Tables 4 and 5.

As shown in Tables 4 and 5, the greatest accuracy for classifying the two groups during the visual perception was 71.87% using the cepstrum coefficient energy, mean, SD, and neural gas classifier. In the case of the mental imagery, the greatest accuracy was 71.25% using the cepstrum coefficient SD and neural gas classifier. The greatest accuracy for classifying the two groups at the resting condition was 85% using the cepstrum coefficient energy and SVM classifier. The average classification accuracies of the two groups using the four cepstrum coefficient parameters were found higher at the resting condition and lower during the mental imagery.

Lastly, the two groups were also classified using the best distinguishing coefficients and the mentioned classifiers. For each feature and state, the channel with the lowest DBI was selected for classifying the two groups. For instance, in the case of visual perception, 4<sup>th</sup> cepstrum coefficient in channel Fp1 was selected for classifying the two groups. Finally, the averaged accuracy (true decision rate) across ten separate classifications was calculated for each feature and state. The obtained results are shown in Table 6.

As shown in Table 6, the greatest accuracies were obtained using SVM classifier. The average classification accuracies were found higher as compared to the obtained average classification accuracies using the four cepstrum coefficient parameters. In addition, the average accuracy of the two groups was higher at the resting condition as compared to the visual perception and the mental imagery.

## Discussion

In this research, the EEG signals of artists and nonartists were analyzed and classified using cepstrum coefficients. It was observed that the cepstrum coefficient parameters were significantly lower for artists as compared to nonartists during the performances of the two cognitive tasks. Real cepstrum is related to power spectrum and power cepstrum is related to average energy of signal.<sup>[36]</sup> Therefore, the decreased cepstrum coefficient energy implies decrease in average energy of EEG for artists. Bhattacharya and Petsche have demonstrated that visual perception of art consists of at least the following three steps: (1) analysis of basic features

such as colors, forms, and shapes, (2) classification of this raw information into coherent and fundamental forms, and (3) giving an appropriate meaning to these fundamental forms using previous knowledge stored in long-term memory. Features such as artistic educational background, personalities, pronounced interest in culture, and good visual memory are involved in step 3. Therefore, such personal qualities acquired by art training influence the performances of visual perception and mental imagery of individuals.<sup>[11]</sup> The mentioned differences between artists and nonartists influence their EEG signals and the EEG features such as the three cepstrum coefficient parameters can reflect them.

The obtained results may be used for measuring progress in novice artists. In this approach, an individual had to carry out the four visual perception tasks and the four mental imagery tasks, and then the cepstrum coefficient parameters are calculated. This experiment is repeated after a period of art training or extensive experiments in art, and then the calculated cepstrum coefficient parameters related to the two experiments are compared. A reduction in the cepstrum coefficient parameters after art training or extensive experiments may imply improved art-related abilities of novice artists. This measuring progress procedure can be improved using the other distinguishable features with the cepstrum coefficient parameters. For instance, Shourie *et al.*<sup>[15,16]</sup> have reported a significant decreased alpha power and a significant increased approximate ENT for artists as compared to nonartists during the performances of the two cognitive tasks. Therefore, a reduction in both alpha power and the cepstrum coefficient parameters and an increase in approximate ENT may be related to improved art-related abilities of novice artists. Result of future researches in various distinguishable features may be used to improve the progress measuring procedure.

A significant decreasing trend in the three cepstrum coefficient parameters has also been found from occipital to frontal brain region for both groups. Therefore, this decreasing trend is related to the task type and is not influenced by artistic expertise. In addition, the trends of changes in the three cepstrum coefficient parameters related to the different regions were similar for the two cognitive tasks. This result is in accordance with the results reported by Kosslyn *et al.*<sup>[37]</sup> and Karkar *et al.*,<sup>[12]</sup> which indicate that visual perception and its mental visualization strongly overlap in terms of their neural resources.

**Table 6: The results of classifying the two groups using the selected cepstrum coefficient and the two classifiers**

CH	Index	Task	ACC%	ACC%
			NG	SVM
Fp1	4	Visual perception	73.75	<b>76.87</b>
O1	7418	Mental imagery	66.87	<b>77.5</b>
O2	1957	Rest	92.5	<b>97.5</b>

The bold entries indicate the most obtained classification accuracy for each of the condition (visual perception, mental imagery and rest).

It was also found that the two groups are distinguishable using the four cepstrum coefficient parameters (energy, mean, SD, and ENT); however, the placement of the electrode is significant in this regard. No considerable difference was found between the four cepstrum coefficient parameters for separating the two groups. A decrease in DBI was also observed at the resting condition, suggesting that the average classification accuracy for the two groups must be higher at rest. The obtained classification accuracies confirm this issue. This result is in accordance with the results reported by Shourie *et al.*,<sup>[13,14]</sup> which indicate that discriminabilities in scaling exponent and wavelet coefficients between the two groups are higher at rest as compared to the performance of similar cognitive tasks.

It was also found that a distinguishing cepstrum coefficient might exist among the cepstrum coefficients, which can separate the two groups despite electrode placement. A decreased DBI was found for the best distinguishing cepstrum coefficient of each channel as compared to the four cepstrum coefficient parameters. Therefore, it is expected that classification accuracy of the two groups must be higher when using the best distinguishable coefficients. The obtained classification accuracies confirm this issue. The greatest accuracies for classifying the two groups during the visual perception and the mental imagery were obtained as 76.87% and 77.5%, suggesting an improved average classification accuracy as compared to the results reported in<sup>[14]</sup> (Shourie *et al.* classified the two groups using wavelet coefficient during the visual perception and the mental imagery with the average accuracy of 75%).

### Acknowledgements

We thank Professor Joydeep Bhattacharya for generously providing us the EEG data.

### Financial support and sponsorship

Nil.

### Conflicts of interest

There are no conflicts of interest.

### References

- Vernon DJ. Can neurofeedback training enhance performance? An evaluation of the evidence with implications for future research. *Appl Psychophysiol Biofeedback* 2005;30:347-64.
- Hatfield BD, Landers DM, Ray WJ. Cognitive processes during self-paced motor performance: An electroencephalographic profile of skilled marksmen. *J Sport Psychol* 1984;6:42-59.
- Haufler AJ, Spalding TW, Santa Maria DL, Hatfield BD. Neuro-cognitive activity during a self-paced visuospatial task: Comparative EEG profiles in marksmen and novice shooters. *Biol Psychol* 2000;53:131-60.
- Crews DJ, Landers DM. Electroencephalographic measures of attentional patterns prior to the golf putt. *Med Sci Sports Exerc* 1993;25:116-26.
- Fink A, Graif B, Neubauer AC. Brain correlates underlying creative thinking: EEG alpha activity in professional vs. novice dancers. *Neuroimage* 2009;46:854-62.
- Wagner MJ. Effect of music and biofeedback on alpha brainwave rhythms and attentiveness. *J Res Music Educ* 1975;23:3-13.
- Wagner MJ. Brainwaves and biofeedback: A brief history – Implications for music research. *J Music Ther* 1975;12:46-58.
- Petsche H, Richter P, Stein AV, Etlinger SC, Filz O. EEG coherence and musical thinking. *Music Percept* 1993;11:117-51.
- Petsche H, Lindner K, Rappelsberger P, Gruber G. The EEG: An adequate method to concretize brain processes elicited by music. *Music Percept* 1988;6:133-59.
- Pang CY, Nadal M, Müller-Paul JS, Rosenberg R, Klein C. Electrophysiological correlates of looking at paintings and its association with art expertise. *Biol Psychol* 2013;93:246-54.
- Bhattacharya J, Petsche H. Shadows of artistry: Cortical synchrony during perception and imagery of visual art. *Brain Res Cogn* 2002;13:179-86.
- Karkare S, Saha G, Bhattacharya J. Investigating long-range correlation properties in EEG during complex cognitive tasks. *Chaos Solitons Fractals* 2009;42:2067-73.
- Shourie N, Firoozabadi SM, Badie K. Information evaluation and classification of scaling exponents of EEG signals corresponding to visual perception, mental imagery & mental rest for artists and non-artists. 18th Iranian Conference of Biomedical Engineering (ICBME). Tehran: IEEE; 2011. p. 156-60.
- Shourie N, Firoozabadi SM, Badie K. A comparative investigation of wavelet families for analysis of EEG signals related to artists and nonartists during visual perception, mental imagery, and rest. *J Neurother Investig Neuromodul Neurofeedback Appl Neurosci* 2013;17:248-57.
- Shourie N, Firoozabadi SM, Badie K. Investigation of EEG alpha rhythm of artists and nonartists during visual perception, mental imagery, and rest. *J Neurother Investig Neuromodul Neurofeedback Appl Neurosci* 2013;17:166-77.
- Shourie N, Firoozabadi M, Badie K. Analysis of EEG signals related to artists and nonartists during visual perception, mental imagery and rest using approximate entropy. *BioMed Res Int* 2014; 2014.
- Johnson AN, Sow D, Biem A, editors. A discriminative approach to EEG seizure detection. *Proceedings of the AMIA Annual Symposium* 2011.
- Kamath C. Comparison of baseline cepstral vector and composite vectors in the automatic seizure detection using probabilistic neural networks. *ISRN Biomed Eng* 2013; 2013.
- Kamath C. Teager energy based filter-bank cepstra in EEG classification for seizure detection using radial basis function neural network. *ISRN Biomed Eng* 2013;2013:1-9.
- Temko A, Nadeu C, Marnane W, Boylan G, Lightbody G. EEG signal description with spectral-envelope-based speech recognition features for detection of neonatal seizures. *IEEE Trans Inf Technol Biomed* 2011;15:839-47.
- Temko A, Boylan G, Marnane W, Lightbody G. Speech recognition features for EEG signal description in detection of neonatal seizures. 32nd Annual International Conference of the IEEE Engineering in Medicine and Biology Society, EMBC'10, September 2010. p. 3281-4.
- Doležal J, Š astný J, Sovka P. Exploiting temporal context in high-resolution movement-related EEG classification. *Radioengineering* 2011;20:666-76.

23. Kim TH, Yoon YG, Uhm J, Jeong DW, Yoon SZ, Park SH. A cepstral analysis based method for quantifying the depth of anesthesia from human EEG. *Conf Proc IEEE Eng Med Biol Soc* 2013;2013:5994-7.
24. Othman M, Wahab A, Khosrowabadi R, editors. MFCC for robust emotion detection using EEG. *Proceedings of the 2009 IEEE 9th Malaysia International Conference on Communications*. Kuala Lumpur, Malaysia: IEEE, December 15–17 2009.
25. Riaz A, Akhtar S, Iftikhar S, Khan AA, Salman A, editors. Inter comparison of classification techniques for vowel speech imagery using EEG sensors. *Proceedings of the 2013 International Conference on Biology, Medical Physics, Medical Chemistry, Biochemistry and Biomedical Engineering*, 2013.
26. Khan T, Westin J, Dougherty M. Cepstral separation difference: A novel approach for speech impairment quantification in Parkinson's disease. *Biocybern Biomed Eng* 2014;34:25-34.
27. Tkach D, Huang H, Kuiken TA. Study of stability of time-domain features for electromyographic pattern recognition. *J Neuroeng Rehabil* 2010; 21.
28. Gupta S, Bansal A. Analysis of ECG signals using cepstrum technique. *National Conference on Computational Instrumentation*, CSIO, Chandigarh, India, March 19-20, 2010.
29. Javdar H, Ripley KL, Arzbacher RC. Power Spectral, and Hartley Analysis of Intracardiac Electrograms for Detection of Tachyarrhythmias. *IEEE*; 1990. p. 175-8.
30. Loon KV, Guiza F, Meyfroidt G, Aerts JM, Ramon J, Blockeel H, *et al*. Prediction of clinical conditions after coronary bypass surgery using dynamic data analysis. *J Med Syst* 2010;34:229-39.
31. Childers DG, Skinner DP, Kemerait RC. The cepstrum: A guide to processing. *Proc IEEE* 1977;65:1428-43.
32. Davies D, Bouldin D. A cluster separation measure. *IEEE Trans Pattern Anal Mach Intell* 1979;1:224-37.
33. Martinetz TM, Schulten KJ. A neural gas network learns topologies. *Artif Neural Netw* 1991:397-402.
34. Fritzke B. Some Competitive Learning Methods. *Systems Biophysics Institute for Neural Network Computation Ruhr-University Bochum*; 1997.
35. Burges C. A tutorial on support vector machines for pattern recognition. *Data Min Knowl Discov* 1998;2:121-67.
36. Hasegawa-Johnson M. *Lecture Notes in Speech Production, Speech Coding, and Speech Recognition*. University of Illinois at Urbana-Champaign; 2000.
37. Kosslyn SM, Ganis G, Thompson WL. Neural foundations of imagery. *Nat Rev Neurosci* 2001;2:635-42.